

# Learning of Frequency-Time Attention Mechanism for Automatic Modulation Recognition

Shangao Lin\*, Yuan Zeng†, and Yi Gong‡

\*Department of Electrical and Electronic Engineering,

Southern University of Science and Technology (SUSTech), Shenzhen, China

†Academy for Advanced Interdisciplinary Studies, SUSTech, Shenzhen, China

‡University Key Laboratory of Advanced Wireless Communications of Guangdong Province, SUSTech, Shenzhen, China

\*linsa2019@mail.sustech.edu.cn, †zengy3@sustech.edu.cn, ‡gongy@sustech.edu.cn

**Abstract**—Recent learning-based image classification and speech recognition approaches make extensive use of attention mechanisms to achieve state-of-the-art recognition power, which demonstrates the effectiveness of attention mechanisms. Motivated by the fact that the frequency and time information of modulated radio signals are crucial for modulation mode recognition, this paper proposes a frequency-time attention mechanism for a convolutional neural network (CNN)-based modulation recognition framework. The proposed frequency-time attention module is designed to learn which channel, frequency and time information is more meaningful in CNN for modulation recognition. We analyze the effectiveness of the proposed frequency-time attention mechanism and compare the proposed method with two existing learning-based methods. Experiments on an open-source modulation recognition dataset show that the recognition performance of the proposed framework is better than those of the framework without frequency-time attention and existing learning-based methods.

**Index Terms**—Modulation recognition, convolutional neural network, frequency-time attention.

## I. INTRODUCTION

Modulation Recognition (MR) is the task of classifying the modulation mode of radio signals received from wireless or wired communication networks. It is an intermediate step between signal detection and signal demodulation. As a step towards understanding what type of communication scheme and emitter is present, MR has been widely used in practical civilian and military applications, such as cognitive radio, spectrum monitoring, communications interference, and electronic countermeasures.

Numerous algorithms for MR have been developed over recent decades. They can be grouped into two categories: likelihood-based (LB) methods and feature-based (FB) methods. LB methods adopt probability, hypothesis testing theory and appropriate decision criteria to classify modulation mode. Although LB methods are optimal in the sense of Bayesian estimation, they rely heavily on prior knowledge and parameter estimation [1]. FB methods perform feature extraction and classification. In the feature extraction step, signal processing

This work is supported in part by National Key R&D Program of China under Grant 2019YFB1802800, Research foundation of Education Bureau of Guangdong under Grant 2019KQNCX128, Guangdong Basic and Applied Basic Research Foundation under Grant 2019B1515130003, Guangdong Science and Technology Program under Grant 2019A1515110479.

algorithms were designed to carefully extract diverse meaningful statistical features, such as high-order statistics (HOS) [2] and cyclostationary characteristics [3]. For the classification, machine learning-based classifiers, including decision tree algorithms [4], support vector machines [5], and artificial neural networks [6], were performed to classify the extracted features. Although FB methods are more robust and effective than LB methods, their recognition performance depends on the quality and amount of manually designed features, which requires knowledge from a limited number of experts and is a time-consuming process.

In the past few years, due to the great success in computer vision and natural language processing, data-driven deep learning methods have also been applied to MR, showing great potential in improving MR accuracy and robustness. Different from traditional MR methods, deep learning-based methods use the deep neural networks (DNNs) to learn from training data by gradient descent, aiming at feature extraction and classification. It can automatically optimize the extracted features for minimizing classification errors. O’Shea *et al.* generated an open modulation recognition dataset, called RadioML2016.10a, using GNU Radio in [8], and first proposed a DNN architecture for MR in [7]. Later, various DNN architectures were introduced to improve the MR accuracy, such as convolutional neural networks (CNNs) [8], recurrent neural networks (RNNs) [9], graph convolutional networks (GCNs) [10], and long-short term memory (LSTM) [11]. These frameworks were directly borrowed from the image or speech recognition areas, but rarely consider the inherent properties of radio signals and communication systems. Recently, a few deep learning-based approaches were proposed to leverage the power of conventional signal analysis algorithms and the classification power of DNNs for MR. For instance, CNNs using frequency-time images generated by Wigner-Ville distribution [12] and signal in-phase and quadrature (IQ) eye diagram [13] as input, were proposed to achieve higher MR accuracy. In [11], HOS of radio signal was computed as an additional signal representation to the CNN classifier. Zeng *et al.* [14] exploited time-frequency analysis of modulated radio signals and proposed an MR approach using the Short-Time Discrete Fourier Transform (STFT) and CNN.

In addition to DNNs, attention mechanisms have also been

used in a wide variety of DNN models, including image classification and speech recognition. This is because a neural attention module can optimize the weights of the input features by minimizing recognition errors. This can hence enhance the important information and reduce the interference caused by irrelevant information in learning-based signal recognition frameworks. In [15], a Squeeze-and-Excitation (SE) attention was proposed. It computes channel attention with the help of 2D global pooling and provides notable performance gains at a considerably low computational cost. In [16], Woo *et al.* proposed a Convolutional Block Attention Module (CBAM), which sequentially implements channel attention and spatial attention to enhance important parts of the input features. In [17], Moritz *et al.* combined connectionist temporal classification and triggered attention to improve the performance of end-to-end speech recognition. In [18], Yu *et al.* proposed a context attention module to explicitly attend on related features at distant spatial locations. Unlike most attention mechanisms in computer vision, including image generation and classification models, which are designed to capture local channel and spatial relations of the input features, attention mechanisms in natural language processing, such as speaker recognition and acoustic event detection, are designed to extract related time and frequency information of the input features.

Inspired by the time-frequency attention mechanisms in natural language processing, in this work, we design a multi-stage attention mechanism to learn useful features from context information in channel, frequency and time dimensions of the corresponding input features. The channel attention is performed first to learn weights regarding channel importance in the input feature map, and then frequency and time attention mechanisms are performed in parallel and composited using learned weights for capturing both frequency and time attention. In addition, we integrate the proposed frequency-time attention module into a CNN-based MR model to improve the performance of MR. Moreover, we conduct ablation experiments to analyze the effectiveness of the designed frequency-time attention mechanism, and compare the proposed MR framework with two existing deep learning-based MR methods in [7] and [19]. Experiment results demonstrate the superior recognition performance of the proposed MR approach.

## II. PROBLEM STATEMENT AND SPECTRUM REPRESENTATION

### A. Problem Statement



Fig. 1: Flowchart of a simple communication system.

This paper considers a simple single-input single-output communication system as shown in Fig. 1, where a symbol is

converted and transmitted to a receiver via a communication channel. The data model of received signal  $r(t)$  is given as:

$$r(t) = \mathcal{F}(s(t)) * h(t) + n(t), \quad (1)$$

where  $s(t)$  denotes the transmission symbol,  $\mathcal{F}$  is a modulation function,  $h(t)$  is the communication channel impulse response, and  $n(t)$  is the additive white Gaussian noise. Given the received signal  $r(t)$ , MR aims at decoding the modulation function  $\mathcal{F}$ . A discrete-time version of the continuous-time signal  $r(t)$  can be obtained by sampling  $r(t)$  for  $n$  times with a sampling rate  $f_s = \frac{1}{T_s}$  i.e.

$$r(n) = r(t)|_{t=nT_s}, -\infty < n < +\infty. \quad (2)$$

### B. Spectrum Representation

Since the time-frequency analysis of a modulated signal can reflect its frequency varies with time, which is an important distinction among different modulated signals. In this work, we exploit the insight from recent work [14] that spectrogram can achieve richer time-frequency representation of the signal, and use short-time Fourier transform (STFT)-based spectrogram to represent the received signal about frequency variation trend with time. The continuous signal  $r(t)$  is first converted to discrete-time signal  $r(n)$  with sampling frequency  $f_s$  as in Eq. (2), and then  $r(n)$  is windowed and transformed into the frequency domain by applying the STFT, that is,

$$R(m, k) = \sum_{n=mK}^{mK+(L-1)} r(n) \omega(n - mK) e^{-j \frac{2\pi k}{L} n}, \quad (3)$$

where  $m$  and  $k$  denote the time frame and frequency bin indices, respectively.  $\omega(n)$  denotes the window function,  $L$  is the frame length, and  $K$  is the frame shift. The spectrogram  $x$  is given as  $x = |R(m, k)|^2$ , where each pixel in spectrogram  $x$  corresponds to a point in frequency and time.

## III. MODULATION RECOGNITION

In this section, we first propose the frequency-time attention (FTA) mechanism for extracting meaningful frequency and time information of the spectrogram inputs. Afterwards, we present a modulation recognition model using CNN and FTA.

### A. Frequency-Time Attention

The overview of the proposed FTA is shown in Fig. 2. The FTA contains three sub-modules, namely Channel Attention Module (CAM), Frequency Attention Module (FAM), and Time Attention Module (TAM). The CAM is used to exploit the inter-channel relationship of features, and extract general information regarding channel importance in the input feature map. The FAM focuses on where is the important frequency information of the channel attention refined feature map, and TAM focuses on where is the important time information of the channel attention refined feature map.

Given an input feature map  $\mathbf{F}$ , FTA first uses CAM  $\mathbf{M}_c$  to generate a channel refined feature map  $\mathbf{F}_c$ . Later, FAM  $\mathbf{M}_f$  and TAM  $\mathbf{M}_t$  are performed on  $\mathbf{F}_c$  in parallel. The parallel attention operations are performed to generate a frequency

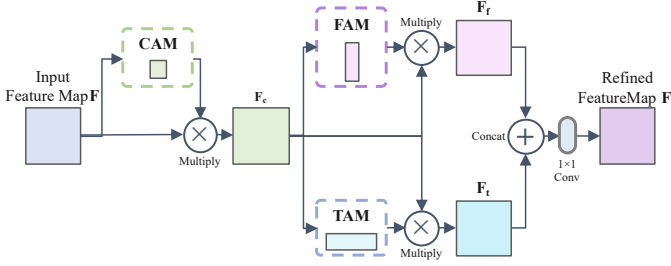


Fig. 2: The overview of the proposed frequency-time attention mechanism (FTA).

refined feature map  $\mathbf{F}_f$  and a time refined feature map  $\mathbf{F}_t$ , respectively. After concatenation of the two refined feature maps  $\mathbf{F}_f$  and  $\mathbf{F}_t$ , a convolution layer with  $1 \times 1$ -sized kernel is applied to generate the final refined feature map  $\mathbf{F}'$ . The overall process of FTA can be summarized as:

$$\begin{aligned} \mathbf{F}_c &= \mathbf{M}_c(\mathbf{F}) \otimes \mathbf{F}, \\ \mathbf{F}_f &= \mathbf{M}_f(\mathbf{F}_c) \otimes \mathbf{F}_c, \\ \mathbf{F}_t &= \mathbf{M}_t(\mathbf{F}_c) \otimes \mathbf{F}_c, \\ \mathbf{F}' &= f^{1 \times 1}([\mathbf{F}_f; \mathbf{F}_t]), \end{aligned} \quad (4)$$

where  $\otimes$  denotes element-wise multiplication.  $f^{1 \times 1}$  denotes a convolutional layer with  $1 \times 1$ -sized kernel. As shown in Fig. 3(a), max-pooling and average-pooling are first performed on the input feature map to generate features that denote two different contexts respectively. The features are then used as the input of a shared network, which consists of a multi-layer perceptron (MLP) comprising two densely connected layers. The outputs of the shared network are element-wise added up. Then a sigmoid function is performed to generate the channel attention map. The channel attention operation  $\mathbf{M}_c$  can be given as:

$$\mathbf{M}_c(\mathbf{F}) = \sigma(MLP(AvgPool(\mathbf{F})) + MLP(MaxPool(\mathbf{F}))), \quad (5)$$

where  $\sigma$  denotes the sigmoid function. The channel attention map is multiplied by the input feature map  $\mathbf{F}$  to generate a channel attention refined feature map  $\mathbf{F}_c$ .

The FAM and TAM have similar procedures. The x-axis of spectrograms represents the time axes, and y-axis represents the frequency axes. The FAM focuses on the frequency axes of input spectrogram and TAM focuses on the time axes. The channel refined feature map  $\mathbf{F}_c \in R^{H \times W \times C}$ , where  $H$  and  $W$  denote the dimension along with the frequency and the time axes, respectively, and  $C$  denotes the number of channels, is the input of FAM and TAM. The FAM averages  $\mathbf{F}_c$  along the time axes to focus on the frequency feature. Specifically, max-pooling and average-pooling are first performed on the frequency feature and then concatenated to further refine the frequency feature. After that, three cascaded  $3 \times 3$  convolutional layers and a sigmoid function are performed to generate a frequency attention map. Unlike FAM, TAM averages  $\mathbf{F}_c$  along the frequency axes to focus on the time feature and

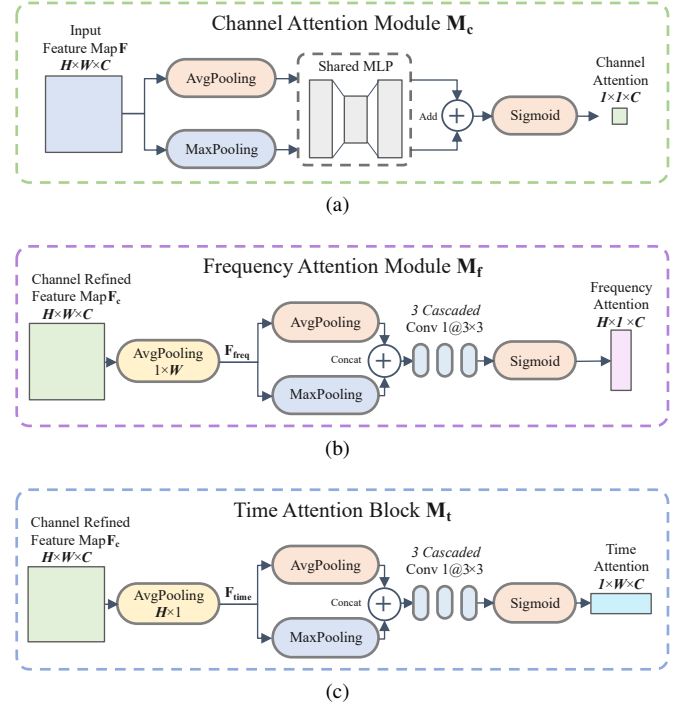


Fig. 3: Flowchart of the three sub-modules in FTA. (a) Channel attention module. (b) Frequency attention module. (c) Time attention module.

performs the same operations as in FAM. The frequency feature  $\mathbf{F}_{freq}$  is given by  $\mathbf{F}_{freq} = AvgPool_{1 \times W}(\mathbf{F}_c)$ , and the time feature  $\mathbf{F}_{time}$  is given by  $\mathbf{F}_{time} = AvgPool_{H \times 1}(\mathbf{F}_c)$ . The frequency attention operation  $\mathbf{M}_f$  and time attention operation  $\mathbf{M}_t$  can then be given as:

$$\begin{aligned} \mathbf{M}_f(\mathbf{F}_c) &= \sigma(f_3^{3 \times 3}([AvgPool(\mathbf{F}_{freq}); MaxPool(\mathbf{F}_{freq})])), \\ \mathbf{M}_t(\mathbf{F}_c) &= \sigma(f_3^{3 \times 3}([AvgPool(\mathbf{F}_{time}); MaxPool(\mathbf{F}_{time})])), \end{aligned} \quad (6)$$

where  $f_3^{3 \times 3}$  denotes 3 cascaded convolutional layers with  $3 \times 3$ -sized kernel. The frequency attention map and time attention map are multiplied by the input feature map  $\mathbf{F}_c$  to generate a frequency refined feature map  $\mathbf{F}_f$  and a time refined feature map  $\mathbf{F}_t$ , respectively. After concatenating  $\mathbf{F}_f$  and  $\mathbf{F}_t$ , a convolutional layer  $f^{1 \times 1}$  is used to generate the final refined feature map  $\mathbf{F}'$ .

## B. Modulation Recognition Network

Fig. 4 illustrates the overview of the proposed MR framework FTA-SCNN, which consists of one input layer, 4 convolutional layers, one densely connected layer, and an output softmax layer. The input of the network is a spectrogram image with the dimension of  $100 \times 100 \times 3$ . The convolutional layers use  $3 \times 3$ -sized kernel and the number of kernels of the 4 convolutional layers is setting as 64, 32, 12, 8. The feature maps generated from each convolutional layer are the input features of FTA, later the refined feature maps of FTA are followed by Rectified Linear Unit (ReLU) [20] and a max-pooling layer with a size of  $2 \times 2$ , except for

the last convolutional layer only followed by ReLU. The densely connected layer consists of 128 neurons. The output of the network is the predicted modulation mode of the input spectrogram image. The network is trained using stochastic gradient descent to minimize the cross-entropy loss function [21], that is,

$$\mathbf{w}^* = \operatorname{argmin}_{\mathbf{W}} \frac{1}{N} \sum_{i=1}^N \mathcal{L}(\mathbf{w}; x^i, t^i), \quad (7)$$

with the number of training examples  $N$ , the true labels  $t^i$ , and the predicted labels  $x^i$ .  $\mathcal{L}$  denotes the loss function, that is,

$$\mathcal{L} = - \sum_j^M \beta_j \log(q_j), \quad (8)$$

where  $M$  denotes the number of classes,  $\beta_j$  is a binary indicator with  $\beta_j = 1$  if  $x^i$  is  $t^i$ , otherwise  $\beta_j = 0$ , and  $q_j$  denotes the predicted probability of belonging to class  $j$ .

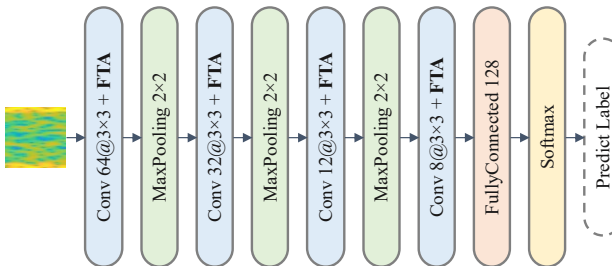


Fig. 4: Network architecture of the proposed FTA-SCNN.

#### IV. EXPERIMENTS

##### A. Dataset

We evaluate the proposed MR framework on an open-source dataset RadioML2016.10a in [22]. RadioML2016.10a consists of analog and digital modulation methods, including 11 commonly used modulations modes in communication systems, which are 8PSK, AM-DSB, AM-SSB, BPSK, CPFSK, GFSK, PAM4, QAM16, QAM64, QPSK, and WBFM. The dataset includes 220000 modulated signals with 20 different signal-to-noise ratios (SNRs) ranging from  $-20$ dB to  $18$ dB, and 1000 signals per SNR per modulation mode. Each signal in the dataset consists of complex IQ. To resemble the practical radio communication environments, RadioML2016.10a is generated in harsh simulated propagation conditions, including Additive White Gaussian Noise (AWGN), multi-path fading, sampling rate offset, and center frequency offset. Unlike most deep learning-based MR methods, where IQ information is directly used as two-dimensional signals, we generate one dimensional modulated signal using the given IQ information in RadioML2016.10a. To train, validate and test the learning-based MR models, in our experiments, for each modulation mode per SNR, we randomly select 700 modulated signals as training data, 100 modulated signals as validation data, and 200 modulated signals as test data.

##### B. Experiment Setup

We use three experiments to analyze the effectiveness of the proposed FTA mechanism and the recognition performance of FTA-SCNN. First, we study the effect of different combination modes of the frequency and time attention mechanisms on MR accuracy. Second, using the proposed model with no attention, called SCNN, as a baseline, we evaluate the effect of the designed FTA on MR performance. After that, we compare the proposed MR framework with two existing deep learning-based MR methods:

- IQ-CNN [7]: a CNN-based MR method, which uses IQ information as the input of CNN.
- CLDNN [19]: a Convolutional Long short-term Deep Neural Networks (CLDNN)-based MR method with the optimal number of filters and filter size for MR.

For signal representation, we convert the one-dimensional radio signals into spectrogram images using frame-based STFT, with a 95% overlapping Hamming window and a frame length of 40 samples. The resolution of the input spectrograms is  $100 \times 100 \times 3$ . We normalize all spectrograms before processing, and use Root Mean Square Prop (RMSprop) as the optimizer. The learning rate starts with 0.0005 and is reduced by a factor of 0.1 when validation loss does not drop within 15 epochs. The training process is terminated when validation loss does not drop within 25 epochs, and we save the model with the smallest validation loss. Later, the saved model is used to predict the modulation mode of each test modulated signal. All experiments are implemented using Keras with Tensorflow backbone and NVIDIA RTX 3090 GPU platform. For each SNR, the training of the proposed MR model takes 1 hour. Fig. 5 gives the training process of FTA-SCNN and SCNN including loss versus epoch at  $-2$ dB SNR.

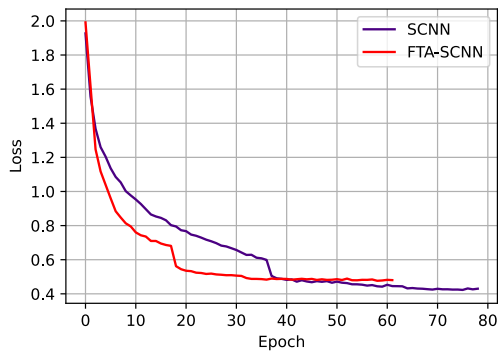


Fig. 5: Training process of FTA-SCNN and SCNN at  $-2$ dB SNR.

##### C. Experiment Results

Table I shows the results of the ablation experiments. The FTA outperforms all other variants by a significant performance improvement. Whether cascaded CAM-FAM or cascaded CAM-TAM, the MR accuracy is improved compared to SCNN without attention, which indicates that the attention

mechanism extracting meaningful frequency or time features can improve MR accuracy. In addition, experiment results in Table I show that cascaded FAM and TAM performs worse than the proposed parallel architecture in FTA. Moreover, compared to CBAM, FTA has a better performance on MR. The ablation study shows that simultaneous modelling of frequency and time importance from spectrograms in CNN improves MR accuracy.

TABLE I: Ablation Experiment Results

Attention Variant	Accuracy (−2dB)	Accuracy (10dB)
None	0.687	0.823
cascaded CAM-FAM	0.694	0.841
cascaded CAM-TAM	0.729	0.834
cascaded CAM-FAM-TAM	0.725	0.843
CBAM [16]	0.733	0.846
proposed FTA	<b>0.766</b>	<b>0.857</b>

Fig. 6 shows the recognition accuracy comparison between SCNN and FTA-SCNN versus SNR. Compared to the baseline model SCNN, the proposed FTA-SCNN has higher MR accuracy. Specifically, the recognition accuracy of FTA-SCNN is around 2% higher than those of the SCNN when SNR is above 10dB. The FTA-SCNN gets around 5% to 8% higher accuracy than SCNN when SNR is between −8dB and 10dB.

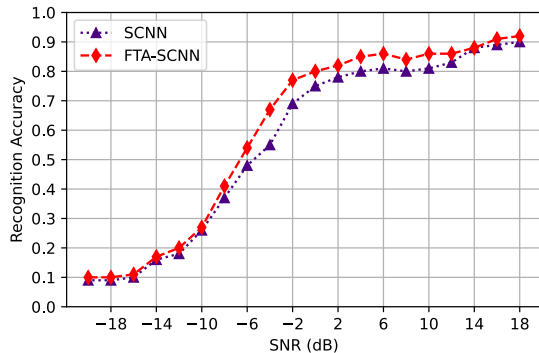


Fig. 6: Recognition accuracy comparison between the FTA-SCNN and SCNN versus SNR.

Fig. 7 shows a series of confusion matrices of FTA-SCNN and SCNN at −2dB and 10dB SNRs. Confusion matrices at −2dB demonstrate that FTA is able to improve the MR accuracy of all modulation modes at low SNRs, especially, MR accuracy of 8PSK, AM-DSB, and GFSK is improved by 15% to 24%. Moreover, confusion matrices at 10dB show that at high SNRs, FTA is still able to improve the MR accuracy of most modulation modes, such as 8PSK, AM-DSB, BPSK, and QPSK. However, the accuracy of WBFM drops by 7% due to the confusion problem between WBFM and AM-DSB. Both of them belong to analog modulation, and the data of WBFM and AM-DSB were generated by the same audio source signals containing silent segments, which makes some of their spectrograms are similar. Another factor that

affects recognition accuracy at 10dB SNR is the confusion problem between 8PSK and QPSK. The reason is that the main difference between 8PSK and QPSK is in phase, while spectrograms are weak in representing phase information.

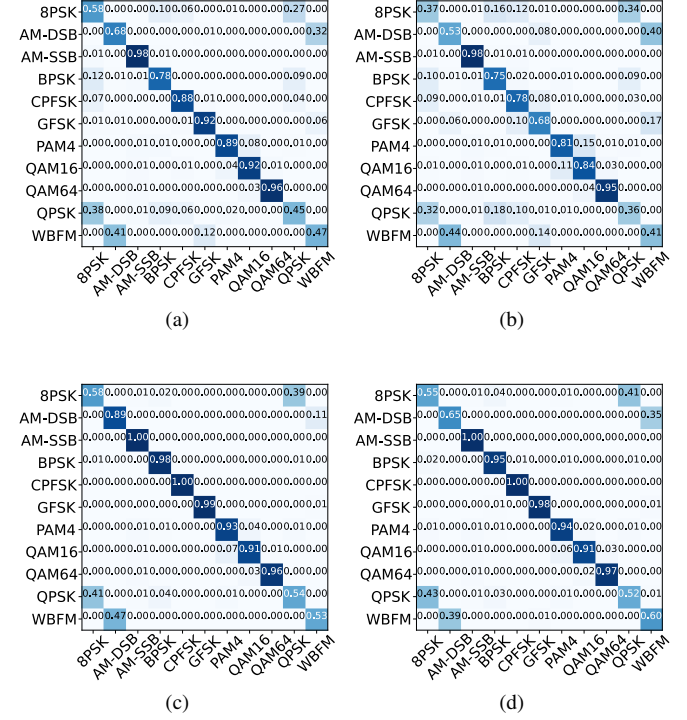


Fig. 7: Confusion matrices of experiment results: (a) confusion matrix of FTA-SCNN at −2dB SNR, (b) confusion matrix of SCNN at −2dB SNR, (c) confusion matrix of FTA-SCNN at 10dB SNR, (d) confusion matrix of SCNN at 10dB SNR.

Next, we compare the MR performance of FTA-SCNN with those of IQCNN and CLDNN. The experiment results are shown in Fig. 8. We observe that FTA-SCNN performs better than both IQCNN and CLDNN. Specifically, FTA-SCNN performs clearly better than other frameworks above −14dB SNR, and it outperforms IQCNN by a significant margin above −4dB SNR. The FTA-SCNN reaches a maximum MR accuracy of 92% at 18dB SNR. For SNRs between −10dB and −2dB, FTA-SCNN still gets around 2% higher accuracy than CLDNN. Fig. 9 shows the feature map visualization of the intermediate process of FTA. It can be observed that some important parts of the input feature  $\mathbf{F}$  are enhanced in the refined feature map  $\mathbf{F}'$  by the proposed FTA mechanism.

## V. CONCLUSION

In this work, we presented a learning-based modulation recognition framework and introduced our baseline CNN model as well as the full model with a novel frequency-time attention (FTA) mechanism. The proposed FTA mechanism consists of Channel Attention Module (CAM), Frequency Attention Module (FAM), and Time Attention Module (TAM),

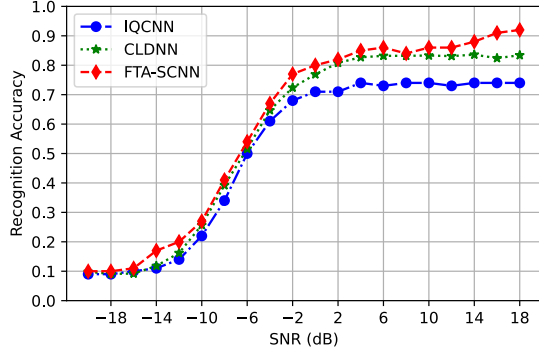


Fig. 8: Recognition accuracy comparison between the FTA-SCNN, CLDNN and IQCNN versus SNR.

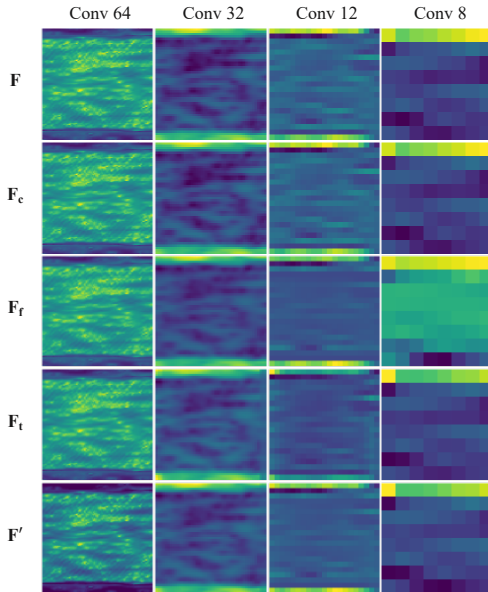


Fig. 9: Feature map visualization of the intermediate process of FTA. From top to bottom, input feature map  $\mathbf{F}$ , CAM refined feature map  $\mathbf{F}_c$ , FAM refined feature map  $\mathbf{F}_f$ , TAM refined feature map  $\mathbf{F}_t$ , and output refined feature map  $\mathbf{F}'$ .

and it is performed on input feature maps to generate attention refined feature maps. We showed that FTA significantly improves modulation recognition results by learning feature representations for explicitly attending to important channel, frequency, and time information. Experiment results demonstrated the effectiveness of modelling FTA in the CNN front-end, as well as simultaneously modelling frequency and time attention, which improves modulation recognition performance. Experiments on the comparison between the proposed FTA-CNN framework and two deep learning-based methods (IQCNN and CLDNN) from literature demonstrated the better recognition capability of the proposed FTA-CNN. As future work, we plan to extend the method to improve recognition performance at low-level SNR using ideas of

deep learning-based signal enhancement or noise reduction. The proposed modulation recognition framework can also be applied to emitter detection, radio signal classification, radio frequency identification, and many others.

## REFERENCES

- [1] W. Wei and J. M. Mendel, "Maximum-likelihood classification for digital amplitude-phase modulations," *IEEE transactions on Communications*, vol. 48, no. 2, pp. 189–193, 2000.
- [2] A. Swami and B. M. Sadler, "Hierarchical digital modulation classification using cumulants," *IEEE Transactions on communications*, vol. 48, no. 3, pp. 416–429, 2000.
- [3] L. Hong, "Classification of bpsk and qpsk signals in fading environment using the ica technique," in *Proceedings of the Thirty-Seventh Southeastern Symposium on System Theory (SSST)*, 2005, pp. 491–494.
- [4] S. R. Safavian and D. Landgrebe, "A survey of decision tree classifier methodology," *IEEE transactions on systems, man, and cybernetics*, vol. 21, no. 3, pp. 660–674, 1991.
- [5] B. Schölkopf, K. Tsuda, and J. P. Vert, *Advanced Application of Support Vector Machines*. MIT Press, 2004, pp. 275–275.
- [6] R. Lippmann, "An introduction to computing with neural nets," *IEEE Assp magazine*, vol. 4, no. 2, pp. 4–22, 1987.
- [7] T. J. O'Shea, J. Corgan, and T. C. Clancy, "Convolutional radio modulation recognition networks," in *International conference on engineering applications of neural networks*, 2016, pp. 213–226.
- [8] R. Li, L. Li, S. Yang, and S. Li, "Robust automated vhf modulation recognition based on deep convolutional neural networks," *IEEE Communications Letters*, vol. 22, no. 5, pp. 946–949, 2018.
- [9] S. Rajendran, W. Meert, D. Giustiniano, V. Lenders, and S. Pollin, "Deep learning models for wireless signal classification with distributed low-cost spectrum sensors," *IEEE Transactions on Cognitive Communications and Networking*, vol. 4, no. 3, pp. 433–445, 2018.
- [10] Y. Liu, Y. Liu, and C. Yang, "Modulation recognition with graph convolutional network," *IEEE Wireless Communications Letters*, vol. 9, no. 5, pp. 624–627, 2020.
- [11] M. Zhang, Y. Zeng, Z. Han, and Y. Gong, "Automatic modulation recognition using deep learning architectures," in *2018 IEEE 19th International Workshop on Signal Processing Advances in Wireless Communications (SPAWC)*, 2018, pp. 1–5.
- [12] J. Zhang, Y. Li, and J. Yin, "Modulation classification method for frequency modulation signals based on the time–frequency distribution and cnn," *IET Radar, Sonar & Navigation*, vol. 12, no. 2, pp. 244–249, 2017.
- [13] Z. Li and X. Zha, "Modulation recognition based on iq-eyes diagrams and deep learning," in *2019 IEEE 5th International Conference on Computer and Communications (ICCC)*, 2019, pp. 1570–1574.
- [14] Y. Zeng, M. Zhang, F. Han, Y. Gong, and J. Zhang, "Spectrum analysis and convolutional neural network for automatic modulation recognition," *IEEE Wireless Communications Letters*, vol. 8, no. 3, pp. 929–932, 2019.
- [15] J. Hu, L. Shen, and G. Sun, "Squeeze-and-excitation networks," in *Proceedings of the IEEE conference on computer vision and pattern recognition*, 2018, pp. 7132–7141.
- [16] S. Woo, J. Park, J.-Y. Lee, and I. S. Kweon, "Cbam: Convolutional block attention module," in *Proceedings of the European conference on computer vision (ECCV)*, 2018, pp. 3–19.
- [17] N. Moritz, T. Hori, and J. L. Roux, "Semi-supervised speech recognition via graph-based temporal classification," *arXiv preprint arXiv:2010.15653*, 2020.
- [18] J. Yu, Z. Lin, J. Yang, X. Shen, X. Lu, and T. S. Huang, "Generative image inpainting with contextual attention," in *Proceedings of the IEEE conference on computer vision and pattern recognition*, 2018, pp. 5505–5514.
- [19] N. E. West and T. O'Shea, "Deep architectures for modulation recognition," in *2017 IEEE International Symposium on Dynamic Spectrum Access Networks (DySPAN)*, 2017, pp. 1–6.
- [20] X. Glorot, A. Bordes, and Y. Bengio, "Deep sparse rectifier neural networks," in *Proceedings of the fourteenth international conference on artificial intelligence and statistics*, 2011, pp. 315–323.
- [21] C. M. Bishop, *Pattern recognition and machine learning*. Springer, 2006.
- [22] T. J. O'shea and N. West, "Radio machine learning dataset generation with gnu radio," in *Proceedings of the GNU Radio Conference*, vol. 1, no. 1, 2016.